Subash Adhikari ✉ 📵 ; Yan Yang 📵 ; William H. Matthaeus 📵 ; Paul A. Cassak 📵 ; Tulasi N. Parashar 📵 ;
Michael A. Shay 📵

Check for updates

View
Online

Export
Citation

Physics of Plasmas

AIP Publishing

Scale filtering analysis of kinetic reconnection and its associated turbulence

View Online   Export Citation   CrossMark

Subash Adhikari,[1,a] [iD] Yan Yang,[2] [iD] William H. Matthaeus,[2] [iD] Paul A. Cassak,[1] [iD] Tulasi N. Parashar,[3] [iD]
and Michael A. Shay[2] [iD]

AFFILIATIONS

[1]Department of Physics and Astronomy and the Center for KINETIC Plasma Physics, West Virginia University, Morgantown,
West Virginia 26506, USA
[2]Department of Physics and Astronomy, University of Delaware, Newark, Delaware 19716, USA
[3]School of Chemical and Physical Sciences, Victoria University of Wellington, Wellington 6012, New Zealand

[a]Author to whom correspondence should be addressed: subash.adhikari@mail.wvu.edu

ABSTRACT

Previously, using an incompressible von Kármán–Howarth formalism, the behavior of cross-scale energy transfer in magnetic reconnection and turbulence was found to be essentially identical to each other, independent of an external magnetic (guide) field, in the inertial and energy-containing ranges [Adhikari *et al.*, Phys. Plasmas 30, 082904 (2023)]. However, this description did not account for the energy transfer in the dissipation range for kinetic plasmas. In this Letter, we adopt a scale-filtering approach to investigate this previously unaccounted-for energy transfer channel in reconnection. Using kinetic particle-in-cell simulations of antiparallel and component reconnection, we show that the pressure–strain interaction becomes important at scales smaller than the ion inertial length, where the nonlinear energy transfer term drops off. Also, the presence of a guide field makes a significant difference in the morphology of the scale-filtered energy transfer. These results are consistent with kinetic turbulence simulations, suggesting that the pressure strain interaction is the dominant energy transfer channel between electron scales and ion scales.

A major theme of turbulence theory is the cascade of energy across scales, providing details of the succession of physical interactions that lead from large-scale energy input to small-scale dissipation and production of internal energy. This energy transfer[1] is either studied in spectral space as a triadic interaction[2–4] or in terms of spatial separation between two physical quantities using the dynamical evolution of the second-order correlation tensors associated with the energy contained in the system.[5–7] The latter approach is quantified using the well-known von Kármán–Howarth (vKH) equation, which was applied primarily to hydrodynamic turbulence and in recent years has been generalized to account for plasma turbulence,[8–11] including compressible magnetohydrodynamic (MHD) and its extensions.[11–14]

The vKH equation is a purely fluid construct. As such, it lacks wave–particle interactions, separate contributions from ions and electrons, and other kinetic effects. We anticipate that the vKH equation based on fluid models remains credible for a kinetic plasma only at scales large enough to be well separated from kinetic effects, namely, the inertial and energy-containing ranges. Using an incompressible

vKH analysis of magnetic reconnection, we showed that the energy transfer characteristics in reconnection at MHD scales are qualitatively similar to those of a decaying turbulence across different scales.[15,16] However, one of the deficiencies in the fluid description is the lack of a known form of dissipation for kinetic plasmas. As a result, a proper description of energy conversion and transfer at scales beyond the inertial range was missing.

In addition to the description in terms of correlations, energy and energy flux distribution across different length scales can also be defined by a scale-filtering operation. Recently, Yang *et al.*[17] also showed that the scale-by-scale energy budget analysis using the vKH approach for a simulation of turbulence agrees with the scale-filtered energy equation resulting from the Vlasov–Maxwell equations in the inertial and energy-containing ranges. Moreover, the scale-filtered energy equation contains the scale-decomposed energy budget of the full Vlasov–Maxwell model. Therefore, the scale-filtering approach can include the physics of energy transfer in Vlasov–Maxwell systems at scales not covered in the vKH formalism, thus providing a more complete picture. In a slightly different approach, Manzini *et al.*[18] showed

that the energy transfer using scale filtering resembles with the vKH analysis in turbulent plasmas.

Scale filtering[19] is based on a properly defined filtering kernel $G_\ell = \ell^{-d} G(\mathbf{r}/\ell)$, which only maintains information about length scales $\geq \ell$. Here, $G(\mathbf{r})$ is a non-negative normalized boxcar window function satisfying $\int d^d r G(\mathbf{r}) = 1$, and d is the number of dimensions of the system. For any field $f(\mathbf{x}, t)$, the scale-filtered field $\overline{f}_\ell(\mathbf{x}, t)$ is defined as

$$\overline{f}_\ell(\mathbf{x}, t) = \int d^d r G_\ell(\mathbf{r}) f(\mathbf{x} + \mathbf{r}, t). \quad (1)$$

Likewise, the density-weighted filtered $f(\mathbf{x}, t)$, also called the Favre-filtered field,[20,21] is defined as

$$\widetilde{f}_\ell(\mathbf{x}, t) = \frac{\overline{[\rho(\mathbf{x}, t) f(\mathbf{x}, t)]_\ell}}{\overline{\rho}_\ell(\mathbf{x}, t)}, \quad (2)$$

where $\rho(\mathbf{x}.t)$ is the density. Following the scale-filtering operation of the Vlasov–Maxwell equations, one can combine the electromagnetic energy, the total bulk flow energy, and the sub-grid scale energy flux to the pressure–strain interaction[17,22,23] as

$$\underbrace{\partial_t \left\langle \sum_\alpha \widetilde{E}_\alpha^f + \overline{E}^m \right\rangle}_{T_f - \varepsilon} = \underbrace{-\left\langle \sum_\alpha (\Pi_\alpha^{uu} + \Pi_\alpha^{bb}) \right\rangle}_{-F_f} \underbrace{-\left\langle \sum_\alpha \Phi_\alpha^{uT} \right\rangle}_{-D_f}, \quad (3)$$

where α represents the plasma species; $\widetilde{E}_\alpha^f = \frac{1}{2} \overline{\rho}_\alpha \widetilde{\mathbf{u}}_\alpha^2$ is the filtered bulk flow ($\mathbf{u}_\alpha$) energy density; $\overline{E}^m = \frac{1}{8\pi}(\overline{\mathbf{B}}^2 + \overline{\mathbf{E}}^2)$ is the filtered electromagnetic energy density; and $\Pi_\alpha^{uu} = -(\overline{\rho}_\alpha \widetilde{\tau}_\alpha^u \cdot \nabla) \cdot \widetilde{\mathbf{u}}_\alpha - \frac{q_\alpha}{c} \overline{n}_\alpha \widetilde{\tau}_\alpha^b \cdot \widetilde{\mathbf{u}}_\alpha$ is the sub-grid scale flux term for bulk flow energy across scales due to nonlinearities, where q_α is the charge of plasma species α, $\widetilde{\tau}_\alpha^u = \widetilde{\mathbf{u}_\alpha \mathbf{u}_\alpha} - \widetilde{\mathbf{u}}_\alpha \widetilde{\mathbf{u}}_\alpha$, $\widetilde{\tau}_\alpha^b = \widetilde{\mathbf{u}_\alpha \times \mathbf{B}} - \widetilde{\mathbf{u}}_\alpha \times \widetilde{\mathbf{B}}$. Note that $\widetilde{\mathbf{u}_\alpha \times \mathbf{B}}$ is the Favre-filtered form of $\mathbf{u}_\alpha \times \mathbf{B}$ and so on. Similarly, $\Pi_\alpha^{bb} = -q_\alpha \overline{n}_\alpha \widetilde{\tau}_\alpha^e \cdot \widetilde{\mathbf{u}}_\alpha$ represents the sub-grid scale flux term for electromagnetic energy across scales due to nonlinearities, where $\widetilde{\tau}_\alpha^e = \widetilde{\mathbf{E}} - \overline{\mathbf{E}}$; $\Phi_\alpha^{uT} = -(\overline{\mathbf{P}}_\alpha \cdot \nabla) \cdot \widetilde{\mathbf{u}}_\alpha$ is the filtered pressure strain interaction that corresponds to the rate of conversion of flow into internal energy, where $\mathbf{P}_\alpha$ is the pressure tensor and ε is the total dissipation rate.

In kinetic plasmas, where the exact form of dissipation may not be known, the total dissipation rate can be calculated by $\varepsilon = -d\langle \sum_\alpha E_\alpha^f + E^m \rangle / dt = -\partial_t (\langle \sum_\alpha E_\alpha^f + E^m \rangle) - \mathbf{u} \cdot \nabla \langle \sum_\alpha E_\alpha^f + E^m \rangle$.

The first term in Eq. (3) is the local time rate of change of flow and magnetic energy for scales $\geq \ell$. This term vanishes for large enough ℓ and approaches $-\varepsilon$ as $\ell \to 0$. With this property, one can define the time rate of change of energy for scales $< \ell$ as $T_f = \varepsilon + \partial_t \langle \sum_\alpha \widetilde{E}_\alpha^f + \overline{E}^m \rangle$ such that $T_f \to \varepsilon$ at large ℓ and $T_f \to 0$ as $\ell \to 0$. The first term on the right-hand side of Eq. (3), F_f defined as $-\langle \sum_\alpha (\Pi_\alpha^{uu} + \Pi_\alpha^{bb}) \rangle$, is associated with the nonlinear energy flux, while the second term D_f represents the internal energy deposition due to the pressure strain interaction, which is further decomposed as

$$D_f = \sum_\alpha \langle -(\overline{\mathbf{P}}_\alpha \cdot \nabla) \cdot \widetilde{\mathbf{u}}_\alpha \rangle = \sum_\alpha \underbrace{\langle -\overline{p}_\alpha \nabla \cdot \widetilde{\mathbf{u}}_\alpha \rangle}_{\overline{p\theta}_\alpha} \underbrace{-\langle \overline{\Pi}_\alpha : \widetilde{\mathbf{D}}_\alpha \rangle}_{\overline{PiD}_\alpha}, \quad (4)$$

where $p_\alpha = P_{\alpha,ii}/3$, $\Pi_{\alpha,ij} = P_{\alpha,ij} - p_\alpha \delta_{ij}$, and $D_{\alpha,ij} = (\partial_i u_{\alpha,j} + \partial_j u_{\alpha,i})/2 - \nabla \cdot \mathbf{u}_\alpha \delta_{ij}/3$. Finally, using these representations, Eq. (3) can be rewritten in the normalized form ($T_f^* = T_f/\varepsilon$) as

$$T_f^* + F_f^* + D_f^* = 1. \quad (5)$$

For kinetic plasmas, Eq. (5) gives a generalized picture of energy transfer in several ways. On the one hand, unlike other equations based on MHD models (e.g., the vKH equation), Eq. (5) is entirely derived from the Vlasov–Maxwell model and therefore is an ideal candidate to describe its energy characteristics. On the other hand, under certain assumptions, Eq. (5) is analogous to the von Kármán–Howarth equation,[5,6] derived through a completely different pathway using structure functions, based on increments. Both formalisms are expressions of conservation of energy across scales and are composed of different energy transfer terms. One can find the correspondence between individual terms of Eq. (5) and the terms in the von Kármán–Howarth equation: T_f^* is equivalent to the time rate of change of energy within a lag l, F_f^* is equivalent to the nonlinear energy transfer dominant in the inertial range, and D_f^* is equivalent to the visco-resistive dissipation in the MHD description. In a turbulence cascade scenario, different filtered terms are expected to dominate at different length scales: the time derivative term T_f^* reaches the total dissipation rate ε at scales larger than the correlation length and decreases at intermediate scales (roughly the inertial range), where F_f^* should dominate. At the smallest scales, the rate of production of internal energy D_f^* (defined here as dissipation) becomes dominant.

In this paper, we use the scale-filtering approach to investigate the Vlasov–Maxwell picture of scale-to-scale energy transfer in magnetic reconnection using kinetic particle-in-cell (PIC) simulations. We find that the overall behavior of the scale-filtered energy equation in reconnection is similar to that of standard decaying turbulence in all the kinetic, inertial, and energy-containing ranges, with a better separation of scales with an increased guide field. In these systems, the filtered pressure strain interaction accounts for the energy transfer between the ion and electron scales. The remainder of this Letter is organized as follows: first, we provide the details of the reconnection simulations, followed by the results. Finally, we end this Letter with the conclusions and discussions.

In this study, we use five 2.5D kinetic particle-in-cell (PIC) simulations of magnetic reconnection performed using the P3D code.[24] In a 2.5D setup, all the vectors have three components with fluctuations only in the (x,y) plane and no variation in the z direction. These systems only vary by the magnitude of the out-of-plane magnetic (guide) field B_g, which is normalized to the reference magnetic field B_0. The number density is normalized to n_0, while length scales are normalized to the ion inertial length $d_i = \sqrt{m_i c^2/4\pi n_0 e^2}$, time is normalized to the inverse of ion cyclotron frequency $\omega_{ci}^{-1} = (eB_0/m_i c)^{-1}$, and speed is normalized to the ion Alfvén speed $v_A = \sqrt{B_0^2/4\pi m_i n_0}$. Similarly, the electric field is normalized to $E_0 = v_A B_0/c$, and temperature is normalized to $T_0 = \frac{1}{2} m_i v_A^2$.

All the simulations are initialized with a double Harris equilibrium over a periodic square domain of size $L = 204.8 d_i$, and a sinusoidal perturbation of amplitude 0.12 is added to initiate reconnection. These systems have a grid spacing of $\delta x = 0.05 d_i$ with 4096^2 grid points, a time step of $\delta t \omega_{ci} = 0.01$, and 100 particles per cell with a total of 1.68×10^9 particles per species. The mass ratio $m_i/m_e = 25$,

the speed of light $c = 15v_A$, and the electron and ion temperature are initially set to $T_e = 0.25$ and $T_i = 1.25$. The reconnecting field is set to $1B_0$, while the out-of-plane guide field is chosen from $[0, 0.1, 0.5, 1, 2]B_0$. The background density is set to $n_b = 0.2$.

Figure 1 provides an overview of all five simulations, showing the out-of-plane electron velocity v_{ez} for the lower current sheet. Well-developed magnetic islands are visible in each run with different dynamics inside it. At the time of analysis, shown on the right top of each panel in Fig. 1, all the runs have an equal amount of reconnected flux ($\Delta\psi \approx 15$) with slight variation in the island widths. Note that the total energy is well conserved in all of the simulations. For more details on the simulations, refer to Refs. 15, 25, and 26. Next, we discuss the scale-filtered energy analysis in reconnection. In Fig. 2, we plot the individual terms of the scale-filtered energy equation [Eq. (5)] as a function of lag scale. The terms in Eq. (5) are calculated for a total of three time slices centered at the time of analysis (shown in Fig. 1),
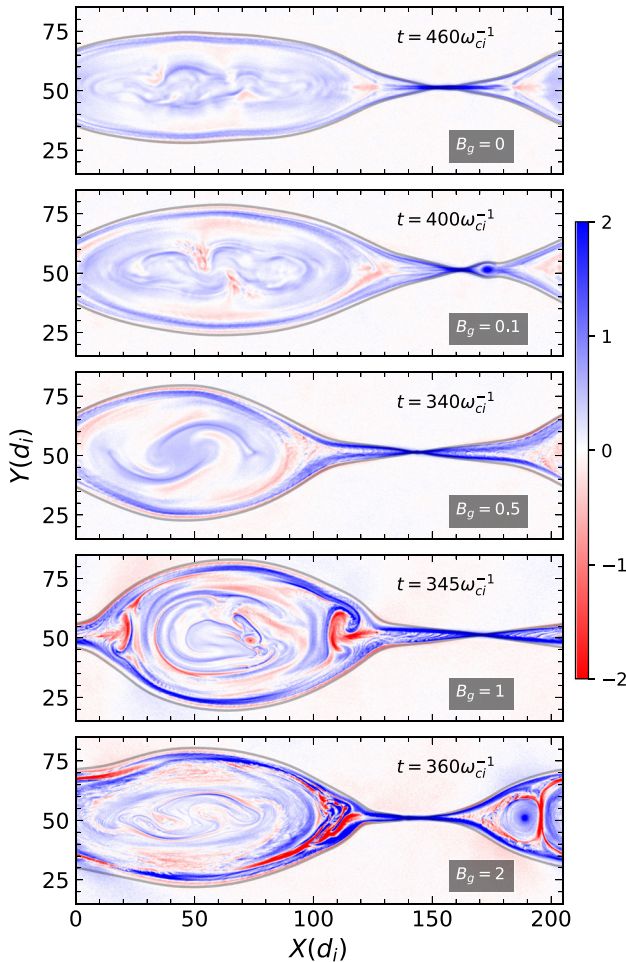
FIG. 1. Overview of the reconnection simulations: out of plane electron velocity v_{ez} in the lower current sheet for each guide field case along with the separatrix, i.e., the contour of the magnetic flux function ψ at the X-line. The time of analysis t is given in the top right of each panel, while the strength of the guide field B_g is given on the bottom right.
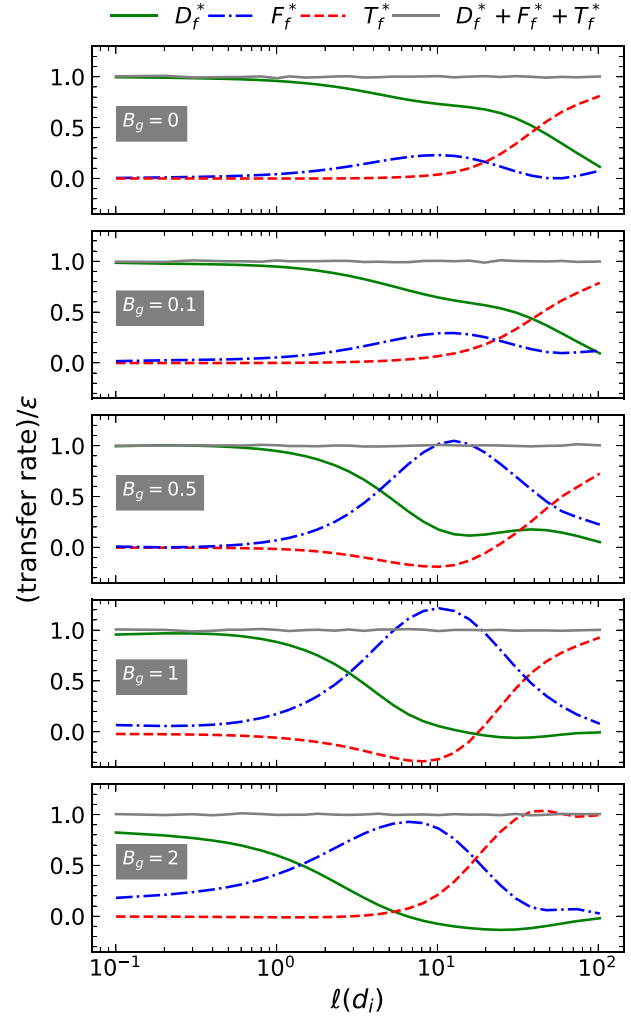
FIG. 2. Individual terms of the scale-filtered energy equation [Eq. (5)] as a function of length scales ℓ for all the reconnection simulations. Each term is normalized to the value of $\varepsilon = -d\langle\sum_\alpha E_\alpha^f + E_m\rangle/dt$ obtained from the simulation. The strength of the guide field used in the simulations is given on the left of each panel.

separated by $\Delta t = 10\omega_{ci}^{-1}$, and the results shown are time-averaged over those three slices.

In all cases studied here, the time derivative term T_f^* is close to the total dissipation rate ε at very large scales and decreases at intermediate scales. While the filtered pressure–strain term D_f^* dominates over the nonlinear energy transfer term F_f^* across all scales for smaller guide field runs ($B_g = 0, 0.1$), F_f^* takes over D_f^* in the inertial scales as the guide field becomes comparable or larger than the reconnecting magnetic field. However, the dominance of D_f^* in the smaller scales still holds. This description of energy transfer at the smaller scales was previously missing in the vKH analysis of reconnection. If one compares this behavior of energy transfer with magnetohydrodynamic (MHD) turbulence, one might argue that D_f^* is identical to the closed form of dissipation in kinetic plasmas. However, since our smallest-filtering window is half of the electron inertial length $d_e/2$, we believe we need
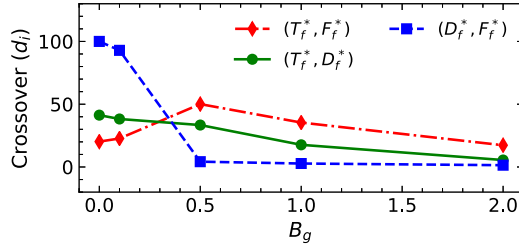
FIG. 3. A comparison of the crossover of the different pairs in Eq. (5) as a function of the guide field B_g.

a much better resolution to understand the dissipation mechanisms at scales smaller than d_e. In any case, for the scales shown, the total energy conversion sums very closely to unity with only a slight fluctuation ($\leq 3\%$), thus accounting for all energy and providing a more complete view of the energy transfer process.

The dominance of F_f^* in the inertial scales with increased guide field is a consequence of a better separation of scales. That is, a well-separated inertial range exists, over which the dynamics is dominated by inertia terms, while the time derivative term and the dissipation term become less prominent and almost negligible. For larger guide fields, the gyroradius of plasma species decreases, confining the electrons and ions closer to the X line. As a result, MHD physics dominates over a larger range extending to smaller scales. This behavior is illustrated in Fig. 3. For the larger guide field cases ($B_g \geq 0.5$), the point of crossover between the scale filtered pressure–strain (PS) interaction D_f^* and nonlinear energy transfer term F_f^* shifts sharply toward the smaller scales allowing F_f^* to dominate the intermediate scales. The crossover between the D_f^* and T_f^* terms also follows a similar trend; however, the shift is relatively less drastic. On the other hand, the crossover between F_f^* and T_f^* terms has a different behavior, which shifts to larger scales until the guide field reaches $B_g = 0.5$ and then falls back to the smaller scales. This is because of different correlation lengths for different systems at the time of analysis.

Next, we investigate the pressure–strain interactions of individual species. In Fig. 4, we show the scale-filtered PS interaction D_f^* for electrons (left column), ions (middle column), and the ratio between these two at different lag values (right column). It is observed that at smaller lag scales, the D_f^* term for electrons is smaller than ions for smaller

guide field as seen in the leftmost plot in Fig. 4. However, for the largest guide field case, $(D_f^*)_e$ dominates over $(D_f^*)_i$. At larger scales, D_f^* for both electrons and ions decreases with increasing guide field. This is certainly due to the role played by pressure dilatation $(\overline{p\theta})$ at those scales. An increase in the guide field decreases the compressibility in the system, which reduces the contribution of $\overline{p\theta}$. It is worth mentioning that for electrons, there is a crossover of D_f^* from all the guide fields cases at $\ell \approx 2 - 3d_i$, while for ions, no such crossover is observed. Finally, looking into the contributions to D_f^*, at smaller scales D_f^* is dominated by $\overline{PiD}$ for both ions and electrons (not shown), an effect that becomes more pronounced with increasing guide field. Both incompressible and compressive pressure–strain interactions ($\overline{PiD}$, $\overline{p\theta}$) are stronger for ions compared to electrons at all scales for small guide field cases. This is the opposite of the largest guide field case. A detailed study on this effect is deferred to a later time.

In the right most panel of Fig. 4, we compare the ratio of the filtered PS term of electrons to ions for different lag scales of 0.5, 1, and $\approx 3d_i$. This ratio, a proxy of relative heating, favors proton heating for $B_g \leq 1$, although a slight increase is seen in that range. However, for the stronger guide field ($B_g = 2$), electron heating is clearly favored.

In this paper, we study the behavior of the scale filtered energy equation in kinetic particle-in-cell simulations of both antiparallel and component reconnection. A guide field analysis of the filtered energy transfer equation reveals that for smaller guide fields, the pressure strain term dominates the non-linear energy transfer term across all scales. This is likely due to the limited system size affording insufficient scale separation that is required for strong turbulence and a well-defined inertial range. However, for guide field larger or comparable to the reconnecting field, the pressure strain term becomes reduced in the inertial range, where the nonlinear energy transfer term dominates. This behavior is consistent with previous findings that the turbulence-like properties of reconnection are more pronounced with an external magnetic field.[16] A property worth mentioning is that the nonlinear term (F_f^*) peaks near the full values of the system dissipation rate ε at scales $\sim 10d_i$ in all the runs, suggesting a fully developed turbulence cascade rate, even if only over a small range of lags.

In general, we find that the overall characteristics of the energy transfer equation are found similar to those of a decaying turbulence. This implies that the energy transfer in reconnection indeed resembles to that of turbulence at all scales and reconnection inherently involves
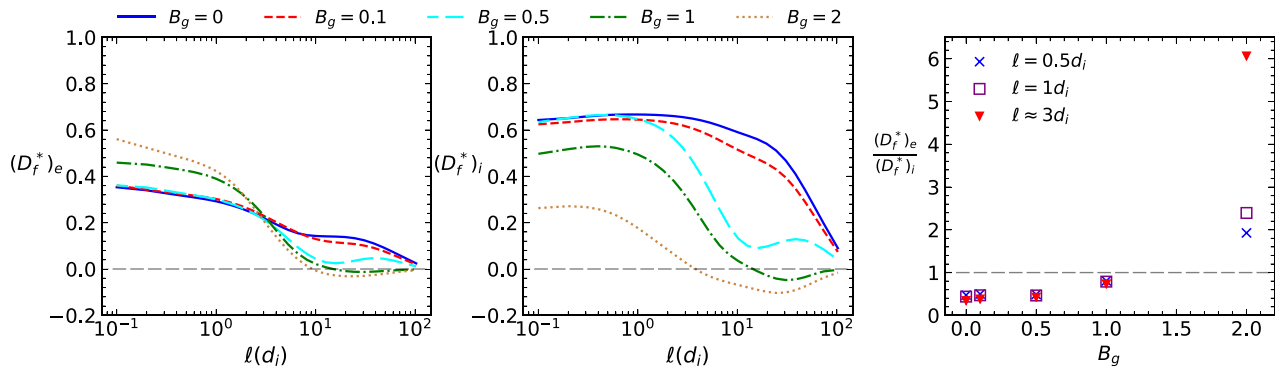

FIG. 4. Scale-filtering analysis of the pressure–strain interaction for electrons (left) and ions (middle) in all the simulations. The right figure shows the scaling of the ratio of the filtered pressure strain interaction of electrons to ions with guide field for lag $\ell = 0.5$, 1, and $\approx 3d_i$.

an energy cascade. We note in passing that different regions in reconnection have different statistical properties including spectral features.[25,27] One could, therefore, anticipate differences in the local behavior of the scale filtered quantities in reconnection, and a future comparison of local energy transfer to turbulence is warranted.

There may be some concerns that the present result may not be fully applicable to realistic 3D systems. Indeed, differences may be anticipated between 2.5D and 3D systems. However, there is published evidence that 2.5D captures at least some of the essential energetics both in reconnection and in turbulence; see Karimabadi *et al.*[28] and Wan *et al.*[29,30] In particular, the energy release (J.E) scales quadratically with the intensity of current to reasonable accuracy in several types of 2.5D kinetic simulations and in 3D kinetic simulations[30,31] as well as in MMS observational results.[32,33] In addition, the scale decomposition of energy transfer has been compared with the wavenumber energy spectra for 2.5D PIC turbulence and 3D PIC turbulence.[17] While there are differences in these quantities, overall, the comparisons are remarkably similar. We, therefore, suspect that the same level of similarity in energy transfer would be obtained for 2.5D and 3D versions of the Harris sheet reconnection problem. There are of course known differences between the turbulence in 2.5D and 3D cases with regard to the nature of intermittency and coherent structures, as well as the possibilities for inverse cascade and self-organization by turbulence. However, on balance, it seems reasonable to assert that the 2.5D case captures the essential features of the direct cascade for the kind of 2D initial state that is represented by the standard reconnection problem we study here.

The scale filtered analysis of the energy-budget equation has an advantage over the vKH formalism as it can account for the missing channel of energy transfer and conversion into internal energy at smaller scales that is represented by the filtered pressure–strain interaction.[17]

Present models that employ the vKH formalism assume fluid closures and therefore ignore the higher order physics involving the pressure tensor and its associated kinetic effects.[34] On the other hand, the scale-filtering analysis is based on the Vlasov equation and hence contains the self-consistent description of the production of internal energy (which we designate as "dissipation") via the pressure–strain term. However, one might be skeptical since the lowest filtering scales discussed in the numerical simulations are $\approx d_e$. A much better-resolved simulation is, therefore, needed to explore how the pressure–strain term or other physics would behave below electron length scales. This will shed light on whether the pressure–strain term can account for energy conversion at much smaller scales or some other kinetic physics needs to be explored. For example, it is almost certain that the strongest guide field case must involve sub-electron inertial scale physics based on the lack of convergence of pressure–strain at the smallest scale shown in Fig. 2.

AUTHOR DECLARATIONS
Conflict of Interest

The authors have no conflicts to disclose.

Author Contributions

Subash Adhikari: Conceptualization (equal); Formal analysis (lead); Validation (equal); Visualization (equal); Writing – original draft (equal). **Yan Yang:** Conceptualization (equal); Investigation (equal); Supervision (equal); Validation (equal); Visualization (equal); Writing – review & editing (equal). **William H. Matthaeus:** Conceptualization (equal); Investigation (equal); Supervision (equal); Validation (equal); Writing – review & editing (equal). **Paul Cassak:** Investigation (equal); Supervision (equal); Visualization (equal); Writing – review & editing (equal). **Tulasi Nandan Parashar:** Conceptualization (equal); Investigation (equal); Visualization (equal); Writing – review & editing (equal). **Michael Anthony Shay:** Conceptualization (equal); Supervision (equal); Visualization (equal); Writing – review & editing (equal).

DATA AVAILABILITY

The data that support the findings of this study are available from the corresponding author upon reasonable request.

REFERENCES

[1]M. Verma, *Energy Transfers in Fluid Flows: Multiscale and Spectral Perspectives* (Cambridge University Press, 2019).

[2]J. A. Domaradzki and R. S. Rogallo, "Local energy transfer and nonlocal interactions in homogeneous, isotropic turbulence," Phys. Fluids A **2**, 413–426 (1990).

[3]F. Waleffe, "The nature of triad interactions in homogeneous turbulence," Phys. Fluids A **4**, 350–363 (1992).

[4]K. Ohkitani and S. Kida, "Triad interactions in a forced turbulence," Phys. Fluids A **4**, 794–802 (1992).

[5]T. De Karman and L. Howarth, "On the statistical theory of isotropic turbulence," Proc. R. Soc. London, Ser. A **164**, 192–215 (1938).

[6]A. Monin and A. Yaglom, *Statistical Fluid Mechanics: Mechanics of Turbulence* (Dover Publications, Inc., 1975), Vol. II.

[7]H. Politano and A. Pouquet, "Dynamical length scales for turbulent magnetized flows," Geophys. Res. Lett. **25**, 273–276, https://doi.org/10.1029/97GL03642 (1998).

[8]S. Galtier, "von Kármán–Howarth equations for Hall magnetohydrodynamic flows," Phys. Rev. E **77**, 015302 (2008).

[9]S. Banerjee and S. Galtier, "Exact relation with two-point correlation functions and phenomenological approach for compressible magnetohydrodynamic turbulence," Phys. Rev. E **87**, 013019 (2013).

[10]P. Hellinger, A. Verdini, S. Landi, L. Franci, and L. Matteini, "von Kármán–Howarth equation for Hall magnetohydrodynamics: Hybrid simulations," Astrophys. J. Lett. **857**, L19 (2018).

[11]N. Andrés, F. Sahraoui, S. Galtier, L. Z. Hadid, P. Dmitruk, and P. D. Mininni, "Energy cascade rate in isothermal compressible magnetohydrodynamic turbulence," J. Plasma Phys. **84**, 905840404 (2018).

[12]S. Banerjee and N. Andrés, "Scale-to-scale energy transfer rate in compressible two-fluid plasma turbulence," Phys. Rev. E **101**, 043212 (2020).

[13]R. Ferrand, S. Galtier, and F. Sahraoui, "A compact exact law for compressible isothermal Hall magnetohydrodynamic turbulence," J. Plasma Phys. **87**, 905870220 (2021).

[14]P. Simon, "Exact law for compressible pressure-anisotropic magnetohydrodynamic turbulence: Toward linking energy cascade and instabilities," Phys. Rev. E **105**, 055111 (2022).

[15]S. Adhikari, T. N. Parashar, M. A. Shay, W. H. Matthaeus, P. S. Pyakurel, S. Fordin, J. E. Stawarz, and J. P. Eastwood, "Energy transfer in reconnection and turbulence," Phys. Rev. E **104**, 065206 (2021).

[16]S. Adhikari, M. A. Shay, T. N. Parashar, W. H. Matthaeus, P. S. Pyakurel, J. E. Stawarz, and J. P. Eastwood, "Effect of a guide field on the turbulence like properties of magnetic reconnection," Phys. Plasmas **30**, 082904 (2023).

[17]Y. Yang, W. H. Matthaeus, S. Roy, V. Roytershteyn, T. N. Parashar, R. Bandyopadhyay, and M. Wan, "Pressure–strain interaction as the energy dissipation estimate in collisionless plasma," Astrophys. J. **929**, 142 (2022).

[18]D. Manzini, F. Sahraoui, F. Califano, and R. Ferrand, "Local energy transfer and dissipation in incompressible Hall magnetohydrodynamic turbulence: The coarse-graining approach," Phys. Rev. E **106**, 035202 (2022).

[19]M. Germano, "Turbulence: The filtering approach," J. Fluid Mech. **238**, 325–336 (1992).

[20]A. Favre, "Statistical equations of turbulent gases," in *Problems of Hydrodynamics and Continuum Mechanics* (Philadephia SIAM, 1969), pp. 231–266.

[21]H. Aluie, "Scale decomposition in compressible turbulence," Physica D **247**, 54–65 (2013).

[22]Y. Yang, W. H. Matthaeus, T. N. Parashar, C. C. Haggerty, V. Roytershteyn, W. Daughton, M. Wan, Y. Shi, and S. Chen, "Energy transfer, pressure tensor, and heating of kinetic plasma," Phys. Plasmas **24**, 072306 (2017).

[23]W. H. Matthaeus, Y. Yang, M. Wan, T. N. Parashar, R. Bandyopadhyay, A. Chasapis, O. Pezzi, and F. Valentini, "Pathways to dissipation in weakly collisional plasmas," Astrophys. J. **891**, 101 (2020).

[24]A. Zeiler, D. Biskamp, J. Drake, B. Rogers, M. Shay, and M. Scholer, "Three-dimensional particle simulations of collisionless magnetic reconnection," J. Geophys. Res.: Space Phys. **107**, SMP 6-1–SMP 6-9, https://doi.org/10.1029/2001JA000287 (2002).

[25]S. Adhikari, M. Shay, T. Parashar, P. S. Pyakurel, W. Matthaeus, D. Godzieba, J. Stawarz, J. Eastwood, and J. Dahlin, "Reconnection from a turbulence perspective," Phys. Plasmas **27**, 042305 (2020).

[26]S. Adhikari, M. A. Shay, T. N. Parashar, W. H. Matthaeus, P. Sharma Pyakurel, J. E. Stawarz, and J. P. Eastwood, "Reconnection and turbulence: A qualitative approach to their relationship," in EGU General Assembly Conference Abstracts, 2022.

[27]F. Pucci, W. H. Matthaeus, A. Chasapis, S. Servidio, L. Sorriso-Valvo, V. Olshevsky, D. Newman, M. Goldman, and G. Lapenta, "Generation of turbulence in colliding reconnection jets," Astrophys. J. **867**, 10 (2018).

[28]H. Karimabadi, V. Roytershteyn, W. Daughton, and Y.-H. Liu, "Recent evolution in the theory of magnetic reconnection and its connection with turbulence," Microphys. Cosmic Plasmas **47**, 231–247 (2014).

[29]M. Wan, W. Matthaeus, V. Roytershteyn, H. Karimabadi, T. Parashar, P. Wu, and M. Shay, "Intermittent dissipation and heating in 3D kinetic plasma turbulence," Phys. Rev. Lett. **114**, 175002 (2015).

[30]M. Wan, W. Matthaeus, V. Roytershteyn, T. Parashar, P. Wu, and H. Karimabadi, "Intermittency, coherent structures and dissipation in plasma turbulence," Phys. Plasmas **23**, 042307 (2016).

[31]R. Bandyopadhyay, Y. Yang, W. H. Matthaeus, T. N. Parashar, V. Roytershteyn, A. Chasapis, D. Gershman, B. Giles, and J. Burch, "Collisional-like dissipation in collisionless plasmas," Phys. Plasmas **30**, 080702 (2023).

[32]A. Chasapis, W. Matthaeus, T. Parashar, M. Wan, C. Haggerty, C. Pollock, B. Giles, W. Paterson, J. Dorelli, D. Gershman, *et al.*, "In situ observation of intermittent dissipation at kinetic scales in the earth's magnetosheath," Astrophys. J. Lett. **856**, L19 (2018).

[33]X. Li, R. Wang, Q. Huang, Q. Lu, S. Lu, J. Burch, and S. Wang, "Energy conversion and partition in plasma turbulence driven by magnetotail reconnection," Astrophys. J. **936**, 34 (2022).

[34]D. Del Sarto, F. Pegoraro, and F. Califano, "Pressure anisotropy and small spatial scales induced by velocity shear," Phys. Rev. E **93**, 053203 (2016).

[35]Computational and Information Systems Laboratory, *Cheyenne: HPE/SGI ICE XA System* (University Community Computing, 2017).

04 June 2024 17:10:02